

Diabetic Peripheral Neuropathy

Evidence for Apoptosis and Associated Mitochondrial Dysfunction

Shanthi Srinivasan, Martin Stevens, and John W. Wiley

We hypothesized that diabetic sensory neuropathy is associated with activation of apoptosis and concomitant mitochondrial dysfunction. Studies were performed in excised intact and acutely dissociated dorsal root ganglion (DRG) neurons from control and streptozotocin-induced diabetic rats with decreased peripheral nerve conduction velocities (NCV). Apoptosis was increased in acutely dissociated DRG neurons from 3- to 6-week-old diabetic rats. Basal mitochondrial membrane potential ($\Delta\psi$) was significantly more positive in DRG neurons from diabetic rats. Depolarization with glutamate resulted in significantly more positive $\Delta\psi$ and delayed recovery of $\Delta\psi$ in neurons from diabetic rats. Restoration of euglycemia for 2 weeks with insulin implants normalized NCV, $\Delta\psi$, and apoptosis. Intact and acutely dissociated neurons from diabetic rats demonstrated decreased Bcl-2 levels and translocation of cytochrome C from the mitochondria to the cytoplasm. Neither levels of Bax nor levels of Bcl-X_L were altered in diabetic neuropathy. Apoptosis associated with mitochondrial dysfunction may contribute to the pathogenesis of diabetic sensory neuropathy. *Diabetes* 49:1932–1938, 2000

Diabetic neuropathy is the most common form of peripheral neuropathy in the Western world, with similar functional, morphological, and metabolic changes in peripheral nerves documented in both human and animal models of type 1 and type 2 diabetes (1,2). The pathophysiology of diabetic neuropathy remains controversial (3,4). Little is known about the etiology of the loss of peripheral sensory neurons that accompanies diabetic neuropathy. Programmed cell death, or apoptosis, has been implicated in diabetic retinopathy and neuropathy (5,6). Impaired mitochondrial function has been implicated in the promotion of apoptosis (7). Abnormalities in mitochondrial function have been reported in both type 1 and 2 diabetes (8,9). We

hypothesized that apoptosis is involved in the pathogenesis of diabetic sensory neuropathy and that activation of the apoptosis cascade is associated with mitochondrial dysfunction. Specifically, we examined whether mitochondrial dysfunction in diabetic sensory neuropathy was associated with decreased levels of the antiapoptotic protein Bcl-2, translocation of cytochrome C from mitochondria to the cytoplasm, and induction of apoptosis (10,11). Few published studies examine a potential connection between activation of the apoptosis cascade in diabetic neuropathy and impaired mitochondrial function, an observation that would help explain the slow progressive loss of peripheral sensory neurons that accompanies this disorder.

Excitatory amino acids such as glutamate have been implicated in the induction of apoptosis in several neurodegenerative disorders (12–14). We examined the effect of glutamate on mitochondrial membrane potential ($\Delta\psi$) and induction of apoptosis in primary sensory (dorsal root ganglion [DRG]) neurons from control and diabetic rats.

RESEARCH DESIGN AND METHODS

Animal model: streptozotocin-induced diabetic rat. Two-month-old male Sprague-Dawley rats (Charles River, Wilmington, MA) were housed at the Unit for Laboratory Animal Medicine–approved Animal Research Facility at the VA Medical Center. Animals were randomized into three groups: diabetic, diabetic with insulin-mediated normalization of serum glucose levels, and healthy controls. Animals were fasted for 12 h before injection of streptozotocin. Intraperitoneal injection of streptozotocin at a dose of 45 mg/kg caused 80% of animals to become hyperglycemic within 1 week of injection, with blood glucose between 250 and 500 mg/dl. This model demonstrates highly reproducible functional (decreased nerve conduction velocities), morphological, and metabolic changes in peripheral nerves similar to those observed in humans with diabetic neuropathy (15). Experiments were performed 3–6 weeks after confirmation of hyperglycemia. Insulin was administered using LinBit, a sustained-release insulin implant (2 U · day⁻¹ · implant⁻¹) (Lin Shin, Canada). After the animals were anesthetized with ketamine and xylazine, the site for implantation was shaved and treated with Betadine solution. Typically, two implants were placed subcutaneously by making a small incision using a 12-gauge needle and positioning the implants with a trocar and stylet available from Lin Shin. Euglycemia was confirmed by glucose monitoring within 1–2 h after implantation, at ~24 h, and when the animals were killed. Insulin-treated animals were used for experiments after 2 weeks of insulin therapy. Control animals were sham-injected with vehicle. Some diabetic animals were implanted with sham implants.

Reagents. Penicillin, streptomycin, goat serum, and trypsin were obtained from GIBCO Laboratories (Gaithersburg, MD). Collagenase, streptozotocin, trypsin, Trypan blue, and neutral buffered formalin were obtained from Sigma (St. Louis, MO). Tdt (terminal transferase) enzyme, Biotin-conjugated dUTP, and fluorescein isothiocyanate (FITC)-Avidin, were obtained from Boehringer Mannheim Biochemical (Indianapolis, IN). JC-1 (5,5',6,6'-tetracholor-1,1',3,3'-tetraethyl-bezimidazolycarbocyanine iodide) was obtained from Molecular Probes (Eugene, OR).

Tissue preparation. Isolated acutely dissociated thoracic and lumbar DRG neurons were aseptically prepared from rats using techniques described previously (15). Isolated DRG neurons were resuspended in minimal essential medium and plated onto matrigel-coated coverslips. The glucose concentration

From the Department of Internal Medicine, University of Michigan, and Ann Arbor VA Medical Centers, Ann Arbor, Michigan.

Address correspondence and reprint requests to John W. Wiley, MD, University of Michigan GCRC, A7119 UH, Box 0108, 1500 East Medical Center Dr., Ann Arbor, MI 48109. E-mail: jwiley@umich.edu. The present address for S.S. is Metabolism Division, Box 8127, Washington University School of Medicine, 660 S. Euclid Ave., St. Louis, MO 63110.

Received for publication 22 February 2000 and accepted in revised form 24 July 2000.

$\Delta\psi$, mitochondrial membrane potential; DRG, dorsal root ganglion; JC-1, 5,5',6,6'-tetracholor-1,1',3,3'-tetraethyl-bezimidazolycarbocyanine iodide; NCV, nerve conduction velocity; PT, permeability transition; TUNEL, terminal deoxynucleotidyl transferase-mediated dUTP nick end labeling.

of the minimal essential medium used to resuspend DRG neurons harvested from diabetic rats was supplemented to 27.0 mmol/l. No sera or growth factors were added to the culture media. Cells were incubated at 37°C for 2–6 h. All studies were performed on neurons within 6 h after plating.

Mitochondrial membrane potential measurement. Isolated DRG neurons prepared as described above were loaded with JC-1 dye (2.5 µg/ml) for 20 min at 37°C (17,18). Using a confocal laser microscope to visualize intracellular organelles, 590 nm/530 nm ratios were obtained under the following conditions: 1) 30-min basal recording, 2) glutamate-stimulated (10 µmol/l glutamate for 5 min in Mg²⁺-free buffer supplemented with 10 µmol/l glycine), and 3) recovery (defined as return to 65% of basal ratio at 50 min after glutamate washout).

Cell viability. Neuronal viability was assessed in basal control and diabetic DRG neurons. Neurons were exposed to 0.2% Trypan blue for 10 min. The number of Trypan blue positive cells per 200 cells were counted in a blinded manner (19).

Determination and quantitation of apoptosis. Apoptosis was detected using the terminal deoxynucleotidyl transferase-mediated dUTP nick end labeling (TUNEL) method (20). This method is based on the principle that terminal deoxynucleotidyl transferase catalyzes a template-independent addition of deoxynucleotides to the free 3' OH end present in DNA breaks formed during apoptosis. The morphological characteristics of apoptosis detected by this assay and the sensitivity and specificity of the TUNEL method were confirmed in our system using measurement of neuronal DNA content in conjunction with flow cytometry and electron microscopy. The reliability of the TUNEL method for detection of apoptosis was confirmed in our laboratory using *cis*-platinum as a positive control for the induction of apoptosis (21–23). In situ fixation of control and diabetic DRG neurons was performed. Rats were given anesthesia using ketamine and xylazine (20 mg/ml), and the rat left ventricle was cannulated with a 16-gauge needle tube. The left ventricle was perfused with porcine heparin (10 units USP/ml; Sigma), diluted in 0.15 mol/l phosphate-buffered saline (pH 7.3) (1/40 dilution), and perfused at a rate of 15 cc/min followed by ice-cold 4% paraformaldehyde in phosphate-buffered saline at 15 cc/min. Thirty minutes after perfusion with paraformaldehyde, the DRGs were removed and placed in 4% paraformaldehyde. The DRGs were processed and embedded in paraffin, using standard protocols at the clinical pathology department, and 5-µm paraffin sections were obtained. The sections were deparaffinized through standard protocols, and a 20-min serum block (20% goat serum) was performed. Studies were also performed using control and diabetic neurons that were fixed and labeled using the TUNEL method under basal conditions (1 h after removal from animal) and glutamate-stimulated conditions (6 h after exposure to 100 µM glutamate for 30 min at 37°C). Two hundred neurons were counted blinded (one-way), and the positive cells were expressed as a percentage of

total neurons counted. The percentage of neurons undergoing apoptosis was standardized to the total number of neurons attached to the coverslip. The number of necrotic neurons was not subtracted from each group before calculation of the percent of apoptotic neurons. Negative controls received only the label solution without terminal transferase, and the positive controls were slides with confirmed apoptosis provided by the company (Oncogene).

Western blot analysis. For mitochondrial and cytosolic protein extraction, the DRGs were extracted using standard procedures (24,25). Protein extracts were probed by SDS-PAGE using 15% agarose. Polyclonal antibodies against rat Bcl-2 (1:750), Bax (1:500), and Bcl-x_l (1:500) (Santa Cruz) and a monoclonal antibody against rat cytochrome C (1:250 dilution) (PharMingen) were used for Western blot analysis. Immunoblot analysis was performed with the appropriate horseradish peroxidase-conjugated secondary antibody using enhanced chemiluminescence (ECL-Plus) Western blot detection reagents (Amersham). Quantitative Western blot analysis was done by scanning the immunoblot using ImagQuant software in conjunction with the STORM machine (Molecular Dynamics).

Measurement of Bcl-2 by immunohistochemistry. The slides were incubated with primary Bcl-2 antibody (1:20, Santa Cruz) for 2 h at room temperature, followed by secondary anti-rabbit-TRITC antibody for 2 h at room temperature. Images were obtained under confocal microscopy (Bio-Rad).

Electrophysiological measurements. Sciatic-tibial motor nerve conduction velocity (NCV) was measured after induction of anesthesia with intraperitoneal urethane (1–1.2 g/kg). Body temperature was monitored by a rectal probe and maintained at 37°C with a warming pad. Hind-limb skin temperature was also monitored by a thermistor and maintained between 36 and 38°C by radiant heat. The left sciatic-tibial motor conduction system was stimulated proximally at the sciatic notch and distally at the ankle via bipolar electrodes with supramaximal stimuli (8 V) at Hz. The latencies of the compound muscle action potentials were recorded via bipolar electrodes from the first interosseous muscle of the hind paw and measured from the stimulus artifact to the onset of the negative M-wave deflection. Motor NCV was calculated by subtracting the distal latency from the proximal latency, and the result was divided into the distance between the stimulating and recording electrode.

Statistical analysis. The data are summarized as the mean ± SE. Statistical analysis was performed using Student's *t* test or the one-way analysis of variance with appropriate adjustment for nonparametric statistics. All statistics were done using the InSTAT software program. Statistical significance was accepted at the *P* < 0.05 level.

RESULTS

Baseline body weights were similar in all experimental groups. After 4 weeks of hyperglycemia, body weights were

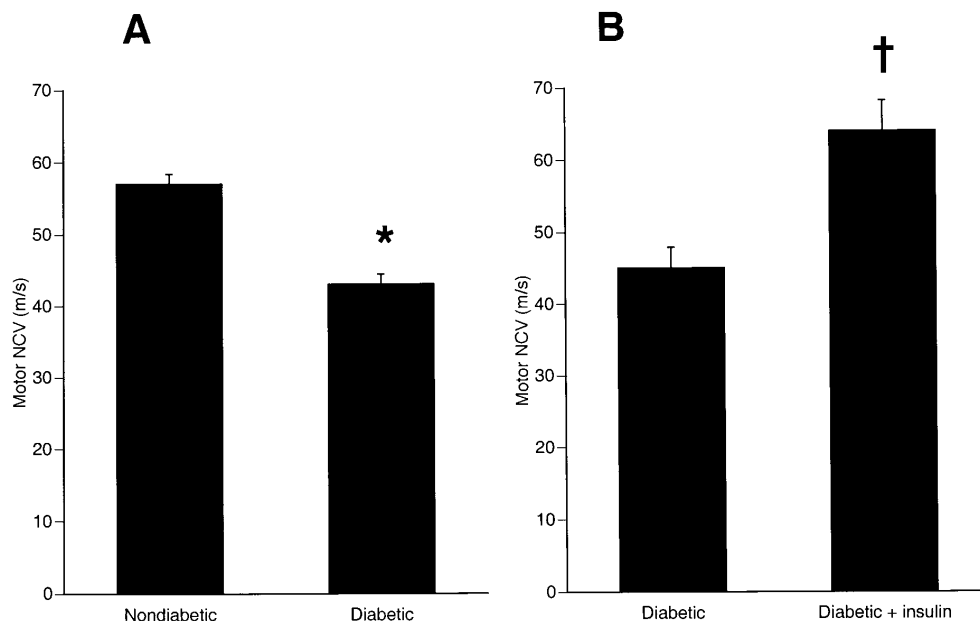


FIG. 1. Effect of streptozotocin-induced diabetes and insulin treatment on NCV. Sciatic motor NCV was determined in nondiabetic (A), untreated streptozotocin-diabetic, and insulin-treated diabetic (B) rats as described in RESEARCH DESIGN AND METHODS. NCV was significantly slower in the diabetic rats. Insulin-mediated euglycemia for 2 weeks normalized the NCV in the treated diabetic rats. **P* < 0.01 vs. nondiabetic rats; †*P* < 0.05 vs. diabetic rats.

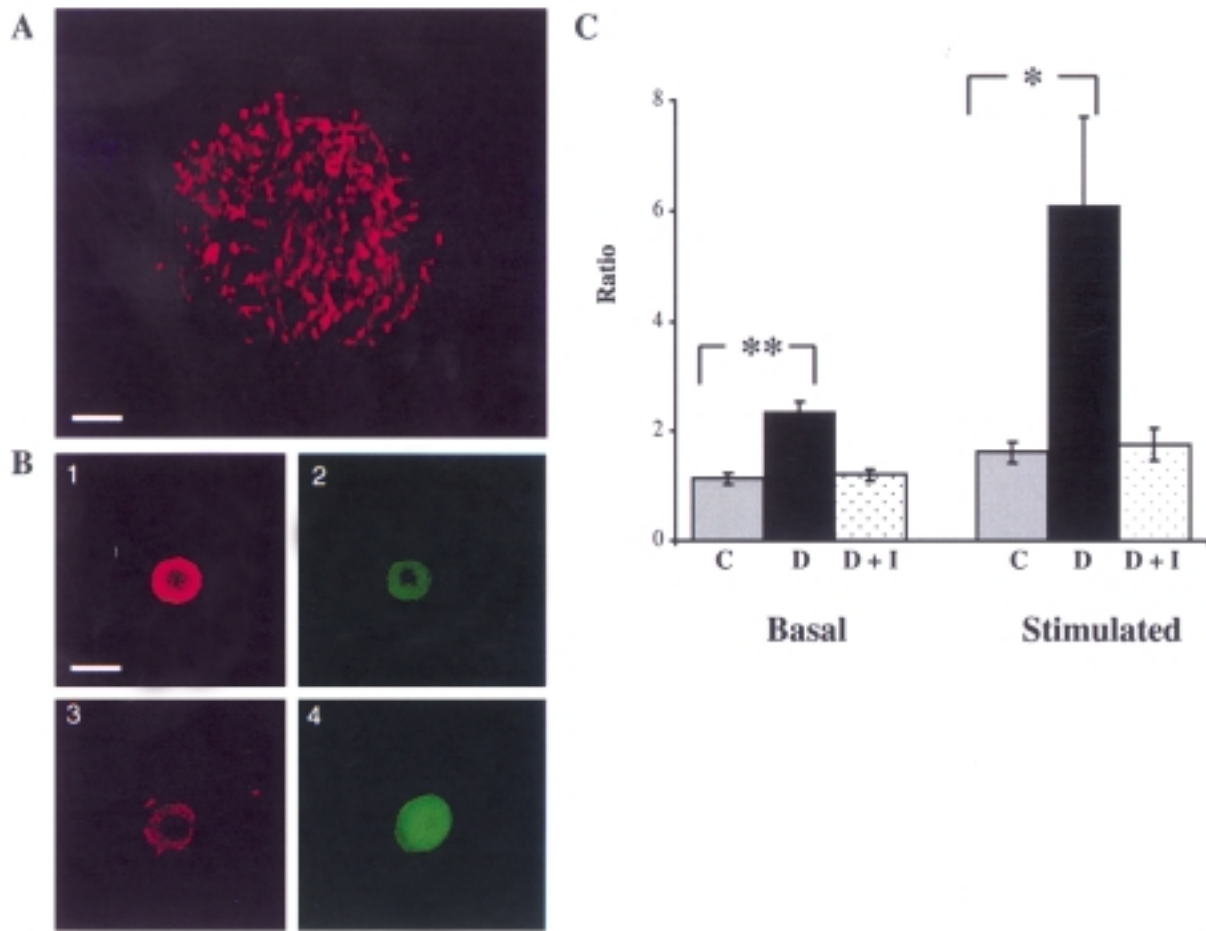


FIG. 2. *A:* Confocal micrograph of mitochondria in a DRG neuron labeled with the JC-1 dye. The rod-shaped mitochondria are labeled with the red J-aggregate (100 \times , 590 nm emission. Bar = 16.5 μ m). *B:* Confocal micrographs of mitochondria in DRG neurons labeled with the JC-1 dye (20 \times) under basal and glutamate-stimulated conditions. Red fluorescence corresponds to J-aggregate fluorescence, and green fluorescence corresponds to monomer fluorescence. Under basal conditions (panels 1 and 2, obtained simultaneously) there is intense red fluorescence with minimal green fluorescence. Stimulation with 10 μ mol/l glutamate for 5 min (panels 3 and 4) results in loss of mitochondrial membrane potential with decreased red fluorescence and increased green fluorescence. Bar = 27.5 μ m. *C:* Mitochondrial membrane potential in control (C), diabetic (D), and insulin-treated diabetic (D+I) rat DRG neurons under basal and stimulated conditions. The *y* axis represents the ratio of green to red fluorescence, with higher ratio corresponding to more positive mitochondrial membrane potentials. The basal $\Delta\psi$ was significantly higher in diabetic neurons (2.34 ± 0.2 , $n = 63$) than in controls (1.13 ± 0.1 , $n = 50$, $P = 0.006$). Stimulation with glutamate augmented this difference: peak ratios were significantly higher in diabetic neurons (6.1 ± 1.6 , $n = 54$) than in control neurons (1.59 ± 0.5 , $n = 35$; $P = 0.02$). Insulin-mediated euglycemia for 2 weeks reversed the abnormalities in mitochondrial $\Delta\psi$ observed in diabetic DRGs. * $P < 0.05$; ** $P < 0.01$.

significantly lower in diabetic rats (270 \pm 15 g) than in controls (378 \pm 12 g, $n = 15$, $P < 0.01$). Plasma glucose levels were markedly higher in diabetic rats (26.2 \pm 1.4 mmol/l) than in controls (7.8 \pm 0.3 mmol/l) ($n = 15$, $P < 0.01$).

Sciatic-tibial motor NCV temporarily decreased in diabetic rats. Sciatic-tibial motor NCV was reduced by 28% ($P < 0.01$) in untreated diabetic rats compared with nondiabetic control rats (Fig. 1A). The decreased NCV was normalized after 2 weeks of insulin-mediated euglycemia (diabetic: 45 \pm 3 m/s; diabetic + insulin: 64 \pm 4 m/s) ($P < 0.05$, $n = 4$) (Fig. 1B).

DRG neurons from diabetic rats demonstrated more positive mitochondrial membrane potentials compared with controls under basal and glutamate-stimulated conditions that were normalized after 2 weeks of euglycemia.

The fluorescent dye JC-1 was used to measure $\Delta\psi$. JC-1 is a cell-permeant dye that exists as an aggregate at the very negative membrane potentials ($\Delta\psi < -100$ mV, red fluorescence, 590 nm) (Fig. 2A). At $\Delta\psi > -100$ mV, JC-1 exists as a

monomer (green fluorescence, 530 nm). Figure 2B shows control neurons at baseline (1 and 2) and during depolarization (3 and 4). The ratio of green/red (530 nm/590 nm) fluorescence can therefore be used as an indicator of mitochondrial membrane potential ($\Delta\psi$) (18,19). $\Delta\psi$ is expressed as a ratio of green (monomer) to red (aggregate) fluorescence. Larger numbers (ratio) correlate with more positive $\Delta\psi$. As shown in Fig. 2C, the baseline $\Delta\psi$ was significantly higher in diabetic (2.34 \pm 0.2, $n = 63$, 3 animals; $P = 0.006$) than in control (1.13 \pm 0.1, $n = 50$, 4 animals) DRG neurons. During depolarization with glutamate (10 μ mol/l for 5 min), peak ratios were significantly higher in diabetic neurons (6.1 \pm 1.6, $n = 54$) than in control neurons (1.59 \pm 0.5, $n = 35$; $P = 0.02$). After 2 weeks of insulin-mediated euglycemia, baseline and glutamate-induced changes in mitochondrial membrane potentials were not significantly different in DRGs from control and treated diabetic rats (baseline: control 1.17 \pm 0.1, $n = 45$, four animals; insulin-treated

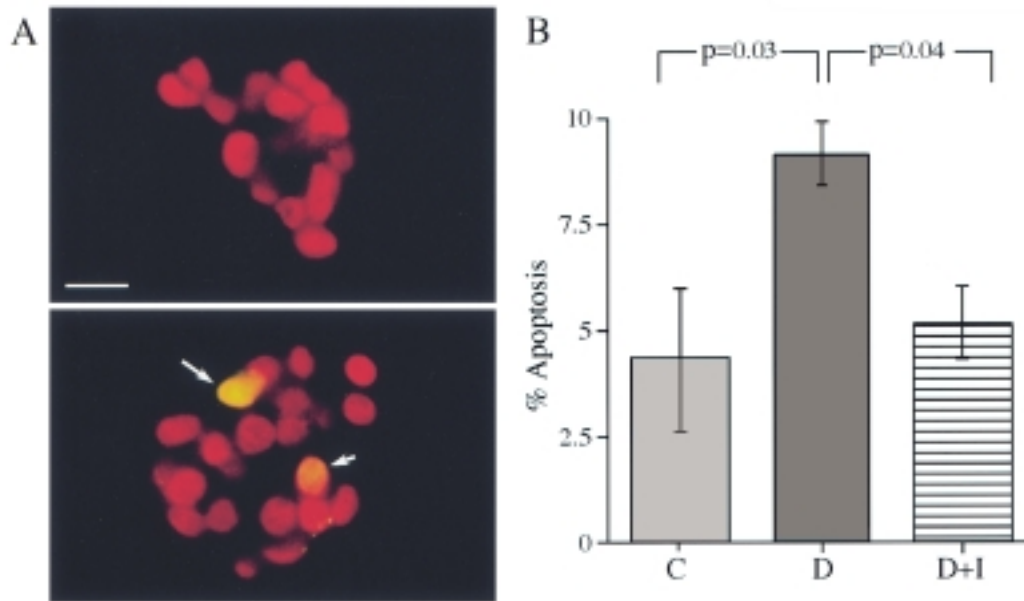


FIG. 3. Apoptosis in control (C), diabetic (D), and insulin-treated diabetic (D+I) rat DRG neurons under basal conditions. **A:** Representative photographs of control (*top*) and diabetic (*bottom*) DRG neurons stained for apoptosis using the TUNEL method, 60 \times magnification. The arrows point to the apoptotic neurons. Bar = 100 μ m. **B:** The mean \pm SE percent of apoptosis in DRG neurons is shown. Basal apoptosis is significantly higher in DRGs from diabetic animals than from controls (control 4.28 ± 1.67 , $n = 6$; and diabetic 9.06 ± 1.05 , $n = 6$; $P < 0.05$). After 2 weeks of euglycemia with insulin therapy, apoptosis levels in diabetic animals were similar to those in controls (insulin-treated diabetic $5.1 \pm 1.3\%$, $n = 5$, $P = 0.04$, compared with untreated diabetic rats).

diabetic 1.20 ± 0.1 , $n = 40$ neurons, four animals; glutamate [10 μ mol/l for 5 min]: control 1.61 ± 0.2 , $n = 46$ neurons, four animals; insulin-treated diabetic 1.75 ± 0.3 , $n = 38$ neurons, four animals, $P > 0.05$). Seventy-five percent of the control neurons recovered compared with 43% of diabetic neurons (recovery defined as return to 65% of baseline ratio 1 h after washout of glutamate).

Increased apoptosis in diabetic DRG neurons reversed after insulin-mediated euglycemia. Apoptosis was measured in acutely dissociated DRGs using the TUNEL method. Two hundred neuronal cells were counted blinded (one-way), and the positive cells were expressed as a percentage of total neurons counted. Basal apoptosis was significantly elevated in DRGs from diabetic animals compared with controls (control 4.28 ± 1.67 , $n = 6$; diabetic 9.06 ± 1.05 , $n = 6$; $P < 0.05$) (Fig. 3A and B). After 2 weeks of euglycemia, the percentage of apoptotic neurons in the insulin-treated diabetic rats was similar to controls (insulin-treated diabetic $5.1 \pm 1.3\%$, $n = 5$; $P = 0.04$ compared with untreated diabetic rats). Sham implants did not affect the percent of apoptotic neurons observed in diabetic rats. Six hours after exposure to glutamate (100 μ mol/l for serum), apoptosis was significantly higher in diabetic than in control neurons (control $5.66 \pm 0.96\%$, $n = 4$; diabetic $12.03 \pm 1.2\%$, $n = 4$; $P < 0.005$). The percent of apoptotic neurons did not increase significantly in the DRGs from diabetic rats exposed to glutamate ($12.03 \pm 1.2\%$) compared with baseline ($9.06 \pm 1.05\%$; $P > 0.05$). In contrast, necrosis measured using Trypan blue exclusion was not different in the baseline and glutamate-stimulated state (baseline: control $14.53 \pm 3.16\%$, $n = 6$, diabetic $9.32 \pm 1.26\%$, $n = 7$, $P > 0.05$; glutamate-stimulated: control $28.7 \pm 2.3\%$, diabetic $19.0 \pm 1.6\%$, $n = 3$, $P > 0.05$). Two hundred neurons were counted blinded (one-way), and the necrotic cells expressed as a percentage of total neurons counted.

Neurons from diabetic rats with neuropathy demonstrated decreased Bcl-2 levels, but no change in Bcl-x_L or Bax levels. We observed a decrease in Bcl-2 levels using quantitative immunohistochemistry and confocal laser microscopy (control 126 ± 10 average pixel intensity, $n = 30$ [Fig. 4A]; diabetic 63 ± 8 average pixel intensity, $n = 10$ [Fig. 4B]; $P < 0.05$). This observation was corroborated with quantitative Western blot analysis. The level of Bcl-2 was lower in diabetic neurons (diabetic $88.5 \pm 4.8\%$ of control average pixel intensity, $n = 8$, $P < 0.05$). Levels of Bcl-x_L and Bax were not significantly different in diabetic neurons compared with controls when measured with quantitative Western blot analysis of whole cell extract (Bcl-x_L: diabetic was $97 \pm 11\%$ of control average pixel intensity, $P = 0.81$, $n = 4$ [Fig. 5A]; Bax: diabetic was $95 \pm 14\%$ of control average pixel intensity, $P = 0.75$, $n = 4$ [Fig. 5B]).

Diabetic neurons demonstrated translocation of cytochrome C from the mitochondria to the cytosol. Cytoplasmic cytochrome C was higher in diabetic neurons than in controls (diabetic $57.97 \pm 13.3\%$ increase over control, $n = 4$, $P < 0.05$) (Fig. 6A). Mitochondrial cytochrome C was significantly lower in neurons from diabetic rats than from controls (diabetic $54.1 \pm 6.5\%$ of control, $n = 8$, $P < 0.005$) (Fig. 6B). This was not due to a generalized decrease in proteins, because α -tubulin was unaffected in diabetic neuropathy.

DISCUSSION

We have demonstrated that the pathophysiology of early sensory neuropathy in diabetes may involve activation of the apoptosis cascade associated with mitochondrial dysfunction. As early as 3 weeks after the induction of diabetes, we observed increased apoptosis associated with elevated (more positive) $\Delta\psi$ in diabetic DRG neurons. Previous reports indicate that the streptozotocin-induced diabetic rat

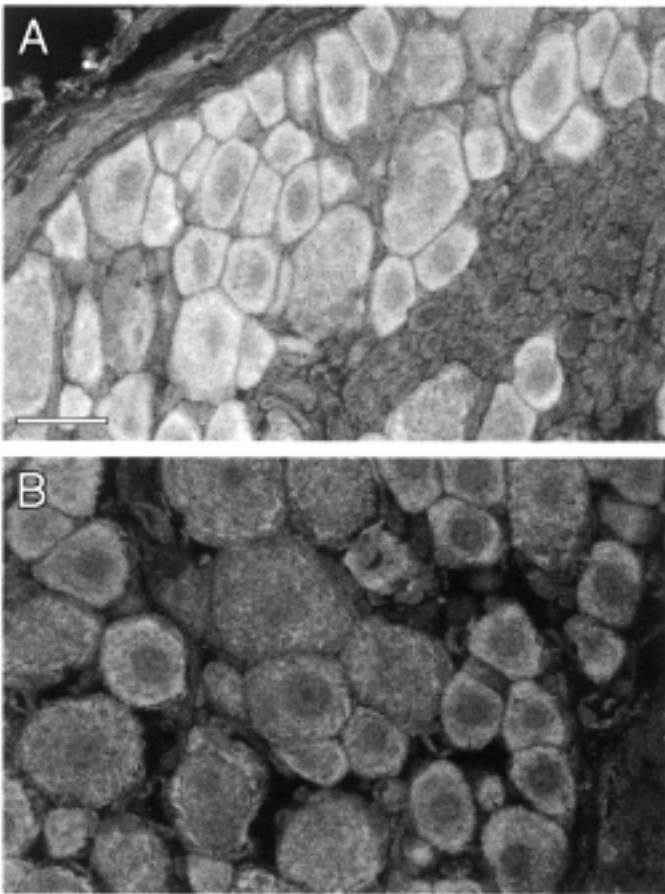


FIG. 4. Immunohistochemistry images of DRG neurons stained for Bcl-2. Representative images of paraffin sections of DRGs fixed in situ and stained for Bcl-2 expression. Images were obtained using confocal microscopy, 60 \times magnification. Diabetic neurons (A) demonstrated decreased Bcl-2 expression under basal conditions using quantitative immunohistochemistry compared to control neurons (B) (control 126 ± 10 pixel intensity, diabetic 63 ± 8 pixel intensity, control $n = 30$, diabetic $n = 10$, $P < 0.05$). Bar = 27.5 μm .

model used in our studies demonstrated functional and morphological features of diabetic peripheral neuropathy (15). We observed that the diabetic rats demonstrated typical features of chronic hyperglycemia, including weight loss and slowing of NCVs. It is not likely that the observed changes in apoptosis, NCV, and $\Delta\psi$ were related to nonspecific streptozotocin toxicity because normalization of serum blood glucose levels with insulin implants for 2 weeks reversed these abnormalities in diabetic rats to control levels. We focused on assessing the reversibility of diabetic neuropathy in early diabetes because previous studies suggest that insulin therapy can prevent the development of retinopathy and peripheral neuropathy (5,26). We believe that this is the first report demonstrating that neuronal apoptosis, mitochondrial dysfunction, and slowing of NCV observed in early diabetic neuropathy can be reversed with restoration of euglycemia for 2 weeks. The mechanism underlying increased apoptosis in diabetic neurons involved decreased levels of Bcl-2 and translocation of mitochondrial cytochrome C to the cytosol. The reduced Bcl-2 levels observed in diabetic neurons may reflect either reduced synthesis or increased proteolysis of this protein.

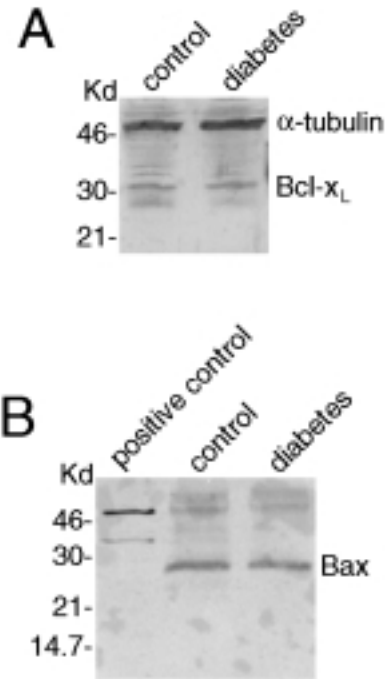


FIG. 5. Bax and Bcl- x_L expression by Western blot analysis under basal conditions. A: There was no difference in the expression of Bcl- x_L in diabetic neurons compared with controls (Bcl- x_L : diabetic $97 \pm 11\%$ of control average pixel intensity, $P = 0.81$, $n = 4$) B: There was no difference in the expression of Bax in diabetic neurons compared with controls (Bax: diabetic neurons $95 \pm 14\%$ of control average pixel intensity, $P = 0.75$, $n = 4$).

Previous studies have reported the presence of apoptosis in diabetic retinopathy and cultured neuroblastoma cells treated with sera from diabetic subjects (5,21,27). Although the percentage of apoptotic neurons in diabetic animals was modest compared to, for example, chemotherapy-induced apoptosis, significant neuronal loss could occur over the typical lengthy course of diabetic neuropathy, explaining the dropout of sensory neurons. Relevant to our observations, the symmetrical loss of sensory neurons over time in diabetic neuropathy is not associated with a significant inflammatory response, which is consistent with activation of apoptosis (2).

The threshold for activation of the apoptotic cascade appears to depend on the ratios and relative abundance of positive and negative regulators, such as expression of the Bcl family of proteins, including Bcl-2, Bax, and Bcl- x_L (28). These proteins are expressed primarily in the inner mitochondrial membrane. Bcl-2 stabilizes the mitochondrial membrane by inhibiting the opening of a large conductance channel known as mitochondrial permeability transition (PT) pore (7) and thereby has an antiapoptotic effect. Opening of the PT pore results in loss of $\Delta\psi$ and expansion of the intermembranous space. This results in outer membrane rupture and the release of caspase-activating enzymes, such as cytochrome C and/or APAF-1, from mitochondria into the cytosol (7). In addition to preventing cytochrome C translocation, evidence suggests that Bcl-2 may protect cells after cytochrome C has been released (29,30). Bcl-2 may also prevent apoptosis by enhancing proton extrusion from mitochondria that helps to maintain the mitochondrial buffering capacity (31).

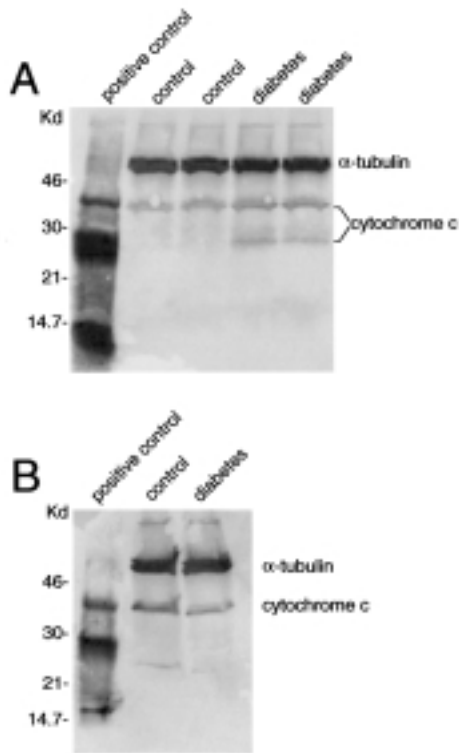


FIG. 6. A: Cytoplasmic cytochrome C was higher in diabetic neurons than in controls (diabetes $57.97 \pm 13.3\%$ increase over control, $n = 4$, $P < 0.05$). α -Tubulin is a cytoskeletal protein that was not affected in diabetic neuropathy. **B:** Mitochondrial cytochrome C was significantly lower in diabetic neurons than in controls (diabetic $54.1 \pm 6.5\%$ of control, $n = 8$, $P < 0.005$).

We also examined the level of the putative antiapoptotic protein Bcl- x_L . Bcl- x_L prevents apoptosis by stabilizing the mitochondrial membrane, similar to the actions of Bcl-2. Like Bcl-2, Bcl- x_L forms channels in the mitochondrial membrane and influences the translocation of cytochrome C to the cytosol through various mechanisms (29). Bcl- x_L has been shown to block apoptosis where Bcl-2 is ineffectual (32). We observed no difference in Bcl- x_L levels in neurons from control and diabetic rats.

Previous studies have implicated increased Bax levels in apoptosis. Bax dimerizes with itself or with Bcl-2 or Bcl- x_L . Recent studies suggest that a shift in the balance toward Bax homodimers enhances apoptosis, whereas the formation of Bcl-2/Bax or Bcl- x_L /Bax heterodimers inhibits programmed cell death (25). Hyperglycemia-induced apoptosis in mouse blastocysts involved increased Bax levels (33). We observed no change in the level of Bax in the diabetic DRG neurons. This is consistent with some studies demonstrating that overexpression of Bax did not increase the apoptosis of DRG neurons following nerve growth factor deprivation (34). Neurotrophin levels are known to be decreased in primary sensory neurons in diabetic neuropathy (35,36). Thus, Bcl-2 and Bax can act independently to inhibit or promote apoptosis, respectively (37). Our studies suggest that diabetic sensory neuropathy is associated with a selective decrease in the levels of Bcl-2. This is an interesting observation that supports selective activation of known participants of the apoptosis cascade in diabetic neuropathy. Additional studies will be

required to delineate the specific components of the apoptotic cascade that are involved in diabetic neuropathy.

Excitatory neurotransmitters such as glutamate have been implicated in the pathophysiology of several models of neurodegenerative diseases (12,13). Of interest, apoptosis was increased by a similar amount in diabetic neurons both before and 6 h after depolarization with glutamate. Therefore, diabetic neurons demonstrated an increased magnitude of mitochondrial depolarization in response to glutamate and delayed recovery, but this was not associated with an increase in apoptosis measured 6 h after the depolarizing event. This result suggests that glutamate-induced depolarization does not contribute to the observed differences in apoptosis between control and diabetic neurons, at least under the experimental conditions used in these studies.

In summary, a selective decrease in Bcl-2 levels in diabetic neuropathy results in loss of $\Delta\psi$, translocation of cytochrome C into the cytosol, and activation of apoptosis. The observed abnormalities in apoptosis, $\Delta\psi$, and NCV were normalized after 2 weeks of insulin-mediated euglycemia. Based on the observation that the apoptosis cascade is activated in diabetic DRG neurons, downstream targets such as caspases may represent potential targets for diagnosis and therapeutic intervention in diabetic neuropathy (38), in addition to insulin-mediated normalization of hyperglycemia.

ACKNOWLEDGMENTS

These studies were supported by supported by National Institutes of Health Grant DK 52387 (J.W.W.), Veterans Administration Merit Award (J.W.W.), and Juvenile Diabetes Foundation International Postdoctoral Fellowship Award (S.S.).

REFERENCES

- Greene DA, Sima AAF, Stevens MJ, Feldman EL, Lattimer SA: Complications: neuropathy, pathogenic considerations. *Diabetes Care* 15:1902–1925, 1992
- Bischoff A: Ultrastructural pathology of peripheral nervous system in early diabetes. In *Vascular and Neurological Changes in Early Diabetes*. New York, Academic Press, 1973, p. 441–449
- Feldman EL, Stevens MJ, Greene DA: Pathogenesis of diabetic neuropathy. *Clin Neurosci* 4:365–370, 1997
- Nathan DM: The pathophysiology of diabetic complications: how much does the glucose hypothesis explain? *Ann Int Med* 124:86–89, 1996
- Barber AJ, Lieth E, Khim SA, Antonetti DA, Buchanan AG, Gardner TW: Neural apoptosis in the retina during experimental and human diabetes: early onset and effect of insulin. *J Clin Invest* 102:783–791, 1998
- Russell JW, Sullivan KA, Windebank AJ, Herrmann DN, Feldman EL: Neurons undergo apoptosis in animal and cell culture models of diabetes. *Neurobiol Dis* 6:347–363, 1999
- Kroemer G, Dallaporta B, Resche-Rigon M: The mitochondrial death/life regulator in apoptosis and necrosis. *Ann Rev Physiol* 60:619–642, 1998
- Mathew CE, Berdanier CD: Noninsulin-dependent diabetes mellitus as a mitochondrial genomic disease. *Proc Soc Exper Biol Med* 219:97–108, 1998
- Schapira AH: Mitochondrial dysfunction in neurodegenerative disorders. *Biochim Biophys Acta* 1366:225–233, 1998
- Marin MC, Fernandez A, Bick RJ, Brisbay S, Buja LM, Snuggs M, McConkey DJ, von Eschenbach AC, Keating MJ, McDonnell TJ: Apoptosis suppression by bcl-2 is correlated with the regulation of nuclear and cytosolic calcium. *Oncogene* 12:2259–2266, 1996
- Marchetti P, Castedo M, Susin SA, Zamzami N, Hirsch T, Macho A, Haeflner A, Hirsch F, Geuskens M, Kroemer G: Mitochondrial permeability transition is a central coordinating event of apoptosis. *J Exp Med* 184:1155–1160, 1996
- White RJ, Reynolds LJ: Mitochondrial depolarization in glutamate-stimulated neurons: an early signal specific to excitotoxic exposure. *J Neurosci* 16:5688–5697, 1996
- Ankarcrona M, Dypbukt JM, Bonfoco E, Zhivotovsky B, Orrenius S, Lipton SA, Nicotera P: Glutamate-induced neuronal death; a succession of necrosis or apoptosis depending on mitochondrial function. *Neuron* 15:961–973, 1995
- Thayer SA, Wang GJ: Glutamate-induced calcium loads: effects on energy metab-

- olism and neuronal viability. *Clin Exper Pharmacol Physiol* 22:303–304, 1995
15. Stevens MJ, Dananberg J, Feldman EL, Lattimer SA, Kamijo M, Thomas TP, Shindo H, Sima AA, Greene DA: The linked roles of nitric oxide, aldose reductase, and (Na⁺, K⁺)-ATPase in the slowing of nerve conduction in the streptozotocin diabetic rat. *J Clin Invest* 94:853–859, 1994
 16. Hall KE, Sima AAF, Wiley J: Voltage-dependent calcium currents are enhanced in dorsal root ganglion neurons from the Bio Bred/Wistar diabetic rat. *J Physiol (Lond)* 486:313–322, 1995
 17. Reers M, Smith TW, Chen LB: J-aggregate formation of a carbocyanine as a quantitative fluorescent indicator of membrane potential. *Biochem* 30:34480–4486, 1991
 18. Cossarizza A, Baccarani-Contri M, Kalshnikova G, Franceschi C: A new method for the cytofluorimetric analysis of mitochondrial membrane potential using the J-aggregate forming lipophilic cation 5,5',6,6'-tetrachloro-1,1',3,3'-tetraethylbenzimidazolcarbocyanine iodide (JC-1). *Biochem Biophys Res Commun* 197:40–45, 1993
 19. Patterson MK: Measurement of growth and viability of cells in culture. *Methods Enzymol* 58:141–152, 1979
 20. Shibasaki F, Mckeon F: Calcinuerin functions in Ca²⁺-activated cell death in mammalian cells. *J Cell Biol* 131:735–743, 1995
 21. Srinivasan S, Stevens MJ, Sheng H, Hall KE, Wiley JW: Serum from patients with type 2 diabetes with neuropathy induces complement-independent, calcium-dependent apoptosis in cultured neuronal cells. *J Clin Invest* 102:1454–1462, 1998
 22. Gold R, Schmied M, Giegerich G, Breitschopf H, Hartung HP, Toyka KV, Lassmann H: Differentiation between cellular apoptosis and necrosis by the combined use of in situ tailing and nick translation techniques. *Lab Invest* 71:219–225, 1994
 23. Cece R, Barajon I, Tredici G: Cisplatin induces apoptosis in SH-SY5Y human neuroblastoma cell line. *Anticancer Res* 15:777–782, 1995
 24. Clark JB, Nicklas WJ: The metabolism of rat brain mitochondria. *J Biol Chem* 245:4724–4731, 1970
 25. Kim CN, Wang X, Huang Y, Ibrado AN, Liu L, Fang G, Bhalla K: Overexpression of Bcl-x_L inhibits Ara-C-induced mitochondrial loss of cytochrome C and other perturbations that activate the molecular cascade of apoptosis. *Cancer Res* 57:3115–3120, 1997
 26. Biessels GJ, Cristino NA, Rutten GJ, Hamers FP, Erkelens DW, Gispen WH: Neurophysiological changes in the central and peripheral nervous system of development and effects of insulin treatment. *Brain* 122:757–768, 1999
 27. Pittenger GL, Liu D, Vinik AI: The apoptotic death of neuroblastoma cells caused by serum from patients with insulin-dependent diabetes and neuropathy may be Fas-mediated. *J Neuroimmunol* 76:153–160, 1997
 28. Basu A, Haldar S: The relationship between Bcl-2, Bax and p53: consequences for cell cycle progression and cell death. *Mol Hum Reprod* 4:1099–1109, 1998
 29. Green DR, Reed JC: Mitochondria and apoptosis. *Science* 281:1309–1312, 1998
 30. Luo X, Budihardjo I, Zou H, Slaughter C, Wang X: Bid, a Bcl2 interacting protein, mediates cytochrome c release from mitochondria in response to activation of cell surface death receptors. *Cell* 94:481–490, 1998
 31. Shimizu S, Eguchi Y, Kamiike W, Funahashi Y, Mignon A, Lacroix V, Matsuda H, Tsujimoto J: Bcl-2 prevents apoptotic mitochondrial dysfunction by regulating proton flux. *Proc Natl Acad Sci U S A* 95:1455–1459, 1998
 32. Gottschalk AR, Boise LH, Thompson CB, Quintans J: Identification of immunosuppressant-induced apoptosis in a murine B-cell line and its prevention by Bcl-x but not Bcl-2. *Proc Natl Acad Sci U S A* 91:7350–7354, 1994
 33. Moley KH, Chi MM, Knudson CM, Korsmeyer SJ, Mueckler MM: Hyperglycemia induces apoptosis in pre-implantation embryos through cell death effector pathways. *Nat Med* 4:1421–1424, 1998
 34. Bernard R, Dieni S, Rees S, Bernard O: Physiological and induced neuronal death are not affected in NSE-*bax* transgenic mice. *J Neurosci Res* 52:247–259, 1998
 35. Unger JW, Klitzsch T, Pera S, Reiter R: Nerve growth factor (NGF) and diabetic neuropathy in the rat: morphological investigations of the sural nerve, dorsal root ganglion, and spinal cord. *Exp Neurol* 153:23–34, 1998
 36. Anand P, Terenghi G, Warner G, Kopelman P, Williams-Chestnut RE, Sincropi DV: The role of endogenous nerve growth factor in human diabetic neuropathy. *Nat Med* 2:703–707, 1996
 37. Knudson CM, Korsmeyer SJ: Bcl-2 and Bax function independently to regulate cell death. *Nat Genet* 16:358–363, 1997
 38. Holtzman DM, Deshmukh M: Caspases: a treatment target for neurodegenerative disease? *Nat Med* 3:954–955, 1997